https://doi.org/10.5194/acp-2022-774
Preprint. Discussion started: 17 November 2022

Atmospheric Chemistry and Physics Discussions

Unambiguous identification of N-containing oxygenated organic molecules using CI-Orbitrap in an eastern Chinese megacity

Yiqun Lu[1,2], Yingge Ma[1], Dan Dan Huang[1], Shengrong Lou[1], Sheng'ao Jing[1], Yaqin Gao[1], Hongli Wang[1], Yanjun Zhang[3], Hui Chen[4], Naiqiang Yan[2], Jianmin Chen[4], Christian George[3], Matthieu Riva[3], Cheng Huang[1]*

[1] State Environmental Protection Key Laboratory of Formation and Prevention of Urban Air Pollution Complex, Shanghai Academy of Environmental Sciences, Shanghai 200233, China;

[2] School of Environmental Science and Engineering, Shanghai Jiao Tong University, Shanghai 200240, China

[3] Univ. Lyon, Université Claude Bernard Lyon1, CNRS, IRCELYON, 69626 Villeurbanne, France;

[4] Shanghai Key Laboratory of Atmospheric Particle Pollution and Prevention (LAP[3]), Department of Environmental Science & Engineering, Jiangwan Campus, Fudan University, Shanghai 200438, China

Corresponding authors: Cheng Huang (huangc@saes.sh.cn)

https://doi.org/10.5194/acp-2022-774
Preprint. Discussion started: 17 November 2022

Atmospheric Chemistry and Physics Discussions

ABSTRACT

Oxygenated organic molecules (OOMs) are dominated by the N-containing species in polluted urban environment. As N-containing OOMs, especially those with more than one nitrogen atoms, prevailed in the high m/z range (m/z > 350Th), unambiguous identification of N-containing OOMs is highly desirable for understanding of their formation processes, precursors and influencing factors. To achieve this, we applied an ultra-high-resolution chemical ionization-orbitrap (CI-Orbitrap) in a field campaign and found that OOMs contain one (1N-OOMs), two (2N-OOMs) and three (3N-OOMs) nitrogen atoms respectively comprised 50%, 26% and 4% of total OOMs. More interestingly, the fraction of 2N-OOMs increased with the increase of carbon number (nC) and were dominated by the ones derived from aliphatic precursors ($2N\text{-}OOM_{Ali}$, 64.2%), indicating the importance of multistep oxidation. Plausible precursors of 2N-OOMs were aliphatics ($2N\text{-}OOM_{Ali}$, 64.2%), aromatics ($2N\text{-}OOM_{Aro}$, 16%), and monoterpenes ($2N\text{-}OOM_{MT}$, 15.4%). The $2N\text{-}OOM_{Ali}$ was the most abundant 2N-OOMs and its fraction even increased in the polluted day with enhanced proportion of the ones with nC>10. While $2N\text{-}OOM_{Ali}$ and $2N\text{-}OOM_{Aro}$ were dominated by daytime photochemical production, nighttime NO_3-initiated oxidation dominated the formation of $2N\text{-}OOM_{MT}$. $2N\text{-}OOM_{Aro}$ were of highest oxygenation level, followed by $2N\text{-}OOM_{MT}$ and $2N\text{-}OOM_{Ali}$, which were affected by photochemistry and NO_x concentrations. These results highlight the significant formation of 2N-OOMs and the influencing factors, on their formation in polluted urban environment, where various VOC precursors and atmospheric oxidants present.

https://doi.org/10.5194/acp-2022-774
Preprint. Discussion started: 17 November 2022

Atmospheric Chemistry and Physics Discussions

1. Introduction

Secondary organic aerosol (SOA) accounts for a significant fraction of particulate matters (Donahue et al., 2009; Ehn et al., 2014; Hallquist et al., 2009; Jimenez et al., 2009). Volatile organic compounds (VOCs) and their oxidation products, *i.e.*, OVOCs, are important precursors of SOA in the atmosphere (Atkinson and Arey, 2003; Bianchi et al., 2019; Ehn et al., 2014; Nie et al., 2022). The N-containing oxygenated organic molecules (OOMs) have been identified as the important products upon VOC oxidation. Especially at high NO_x levels, these products become more dominant while the others (*i.e.*, alcohols, hydroperoxides and RO_2 cross-reaction products) are likely suppressed (Bianchi et al., 2019; Zhao et al., 2018). The nitrogen atoms in OOM molecules are assumed to be mainly associated with nitrate group ($-ONO_2$) formed from bi-molecular reaction between RO_2 radical and NO. Field measurements also observed that up to 54 % of molecules in organic aerosol (OA) contain nitrate functional groups under different atmosphere (Ditto et al., 2020; Lee et al., 2016; Lin et al., 2021; Rollins et al., 2013; Xu et al., 2015; Ye et al., 2021; Yu et al., 2019).

The N-containing OOM molecules can be classified into 1N-OOMs, 2N-OOMs, and 3N-OOMs, according to the number of nitrate functional group in the molecule. The chemical composition of N-containing OOMs is determined by their precursors, formation pathways and NO_x level in the atmosphere (Bianchi et al., 2019; Ehn et al., 2014; Nie et al., 2022; Pye et al., 2019; Riva, 2016; Yan et al., 2016). Recent observations in megacities of China indicated that 2N-OOMs accounted for significant fractions (about 30-33%) among total N-containing OOMs besides 1N-OOMs (66-70%) due to the high NO_x concentrations in polluted urban environment (Nie et al., 2022; Yan et al., 2021). Some laboratory studies also proposed that the potential formation pathways of 2N-OOMs, such as the multiple-step OH oxidation (Garmash et al., 2020) or the NO_3-initiated oxidation followed by NO termination (Kiendler-Scharr et al., 2016; Liebmann et al., 2019), suggesting the increased importance of multi-step bimolecular oxidation in the formation of 2N-OOMs. On the other hand, it was also found that the formation of 2N-OOMs showed the clear preference of specific precursors compared to 1N-OOMs, *i.e.*, significantly higher branch ratio of 2N-OOMs from aliphatic hydrocarbons than those from aromatics (Nie et al., 2022), suggesting

https://doi.org/10.5194/acp-2022-774
Preprint. Discussion started: 17 November 2022


Atmospheric Chemistry and Physics Discussions

considerable difference from 1N-OOMs in terms of formation pathway. Determining the formation pathway of N-containing OOM molecules, especially those containing two to three nitrogen atoms, in real atmosphere, is challenging. Identification of their chemical compositions in molecular level is the key for advancing our understanding in the precursor, formation and sources of N-containing OOMs in polluted atmosphere, where thousands of oxidation products exist and evolve constantly.

Traditionally, a chemical ionization atmospheric pressure interface time-of-flight mass spectrometer (CI-APi-TOF) has been used to measure the gaseous OOMs (Berndt et al., 2016; Ehn et al., 2014; Jokinen et al., 2014; Rissanen et al., 2014). Using a CI-APi-TOF, increasing number of studies have been reporting the formation of OOMs through the oxidation of various VOC precursors in chamber or flow tube (Berndt et al., 2016, 2018; Ehn et al., 2014; Garmash et al., 2020; Jokinen et al., 2014, 2015; Rissanen et al., 2014; Wang et al., 2020; Zhao et al., 2018). While 2N-OOMs in real ambient almost exclusively located in high m/z (mass-to-charge) range (*i.e.*, 300 - 500 Th), a CI-APi-TOF with highest mass resolution of 12,000 (m/Δm, in full width at half maximum), can hardly identify the molecular compositions of 2N-OOMs unambiguously. This is because low mass resolving power imposes significant uncertainties on separating overlapping peaks, which increases rapidly with increasing m/z and decreasing mass resolution. Taken the integer m/z of 342 as an example, multiple peaks overlap at this nominal mass, *i.e.*, $C_7H_8O_{10}N_2(NO_3)^-$ (342.0057 Th), $C_8H_{12}O_9N_2(NO_3)^-$ (342.0421 Th), $C_9H_{16}O_8N_2(NO_3)^-$ (342.0785 Th), $C_{10}H_{20}O_7N_2(NO_3)^-$ (342.1149 Th). The adjacent peaks are of mass differences (Δm) of 0.0364 and a good peak separation of these peaks (4σ) requires mass resolutions of at least 16,000. Therefore, development and application of mass spectrometry techniques with extremely high performance in detection limit, time resolution, and mass resolution, are highly desirable.

To achieve accurate identification of molecular formula from the extremely complex mass spectra, a CI (nitrate) inlet had also been coupled to an orbitrap mass spectrometer (CI-Orbitrap) to measure the OOMs in ultra-high mass resolution (m/Δm> 100,000) (Riva et al., 2019a; Zhang et al., 2022). The ultra-high mass resolving power of CI-Orbitrap will undoubtedly provide significant improvements in molecular identification, separation, and quantification. Herein, we applied a CI-Orbitrap in a field

https://doi.org/10.5194/acp-2022-774
Preprint. Discussion started: 17 November 2022


Atmospheric Chemistry and Physics Discussions

campaign for the measurements of OOMs, with a special focus on 2N-OOMs, in molecular level in urban Shanghai. The site represents a typical eastern Chinese megacity characterized by intense human activities, multiple anthropogenic emissions and high NO_x concentrations. Based on the measurement results as well as our current knowledge on N-containing OOM formation, we classify the observed 2N-OOMs into different precursor groups and explore the potential influencing factors on their formation. Furthermore, supported by positive matrix factorization (PMF), sources and gas-phase oxidation processes for 2N-OOM formation in urban Shanghai were identified.

2. Ambient measurement and methodology

2.1 Measurements

The field campaign was carried out from 31th October to 18th November, 2020 on the top-floor of an 8-story building in Shanghai Academy of Environmental Sciences (31°18' N, 121°43' E), which sits in a densely populated region surrounded by commercial properties and residential dwellings without significant industrial sources nearby. The site can represent a typical urban area of Shanghai affected by severe local emissions from vehicular traffic, commercial, and residential activities. Our campaign was carried out in autumn which represents a typical transition period from strong photochemistry in summer to intense regional transport in winter. At times, air masses transported from the neighboring provinces or even further from the northern China can also affect the air quality of the site.

The 2N-OOMs as well other OOMs molecules were measured in real time with a nitrate-Orbitrap. The operation of nitrate-Orbitrap has been detailed in previous studies as well as in one of our companion studies (Zhang et al., 2022), thus is only briefly described here. Ambient air was drawn into the ionization source through a 1m stainless-steel tube (3/4 inch). The reagent ion was produced by passing nitric acid in sheath flow (20L/min) into a PhotoIonizer (Model L9491, Hamamatsu, Japan) and was then introduced into a co-axial laminar flow reactor, in which the reagent ions interact with the air samples. The charged species were detected by an orbitrap mass analyzer with a mass resolution of about 140,000. Mass-dependent transmission calibrations was also performed using a depletion method (Heinritzi et al., 2016). Other ancillary measurements, including the $PM_{2.5}$ concentrations, trace gases (SO_2, O_3 and NO_x), volatile

https://doi.org/10.5194/acp-2022-774
Preprint. Discussion started: 17 November 2022

Atmospheric Chemistry and Physics Discussions

organic compounds, as well as meteorological parameters (wind direction and speed, solar radiation, etc.) were detailed in Supporting Information (SI-1). An overview of the measurement data, illustrating the air quality as well as the meteorological conditions during the campaign, is provided in SI-2 and Figure S1.

2.2 Data analysis of nitrate CI-Orbitrap

The raw mass spectra were first extracted by Orbitool (Cai et al., 2020) and the molecular information was then achieved by applying a homemade toolkit based on the MATLAB software. The toolkit drew on the idea from "tofTools" package which is used for analyzing the mass spectral data obtained from the TOF analyzer, such as nitrate CI-API-TOF (Junninen et al., 2010). The concentrations of the detected species are then determined as follows:

$$[\boldsymbol{X}] = \frac{\boldsymbol{i}[\boldsymbol{X}^-]}{\boldsymbol{NO_3^-} \cdot (\boldsymbol{HNO_3})_{\boldsymbol{0-2}}} \cdot \boldsymbol{C} \quad (\mathbf{1})$$

where $i[X^-]$ is the transmission-corrected signal intensity of ion X in unit of counts per second (cps), C represents the calibration factor. C is determined from the collision frequency of target species with the nitrate ions (cluster) during its residence in the charger, taking into account of the losses onto the walls of the reactor and the tube (Eq. 2):

$$\boldsymbol{C} = \boldsymbol{C_{H2SO4}} = \frac{\mathbf{1}}{\boldsymbol{k_{ion}} \times \boldsymbol{RT} \times \boldsymbol{f_{inlet}}} \quad (\mathbf{2})$$

where k_{ions} is the ion collision frequency in the range of (1.7 – 2.3) $\times 10^{-9}$ cm^3 s^{-1} (Ehn et al., 2014); RT is the residence time in the charger and f_{inlet} represents the fractions of target species that passed through the inlet.

Herein, we apply the C determined for sulfuric acid (H_2SO_4) of 3.4×10^9 molecules cm^{-3} ncps^{-1} to semi-quantify the concentrations of OOMs, which is widely used in previous studies. Among the low volatility vapors, it had been demonstrated that nitrate ions exhibit highest charging efficiency toward H_2SO_4 (Ehn et al., 2014; Hyttinen et al., 2015, 2018; Riva et al., 2019b). The estimated concentrations of OOMs thus can be considered as the lower limits with an uncertainty of ±50% according to error propagation. Positive matrix factorization (PMF) was also performed for the measured species using Source Finder (SoFi, v6.3) based on Igor and run by the multilinear engine (ME-2) as detailed in SI-S3 and Figure S3-S6 (Canonaco et al., 2013).

https://doi.org/10.5194/acp-2022-774
Preprint. Discussion started: 17 November 2022

Atmospheric Chemistry and Physics Discussions

3. Results and discussion

3.1 Chemical characteristic of OOMs

In total, we have identified 562 OOMs, which concentrated in the nC range of 5 to 10, taking up 84.6% of total OOMs. Possible precursors of $C_{5\text{-}10}$ OOMs include isoprene (C_5), benzene/alkyl benzenes ($C_{6\text{-}10}$), aliphatic VOCs ($C_{5\text{-}10}$) and monoterpene (C_{10}) according to previous studies (Bianchi et al., 2019; Nie et al., 2022). $C_{\leqslant 4}$ OOMs only took up a small fraction of 6.7% among total OOMs and were likely a result of the decomposition from OOMs with large carbon numbers as suggested by one of our companion studies. The rest 8.7% were $C_{>10}$ OOMs which accounted for a dominating fraction (70%, Figure S2) among the extremely low-volatility organic compounds (ELVOC, $C^* < 3 \times 10^{-5}$ μg m^{-3}) (Donahue et al., 2011, 2012; Schervish and Donahue, 2020), and potentially poses larger impacts on SOA formation owing to their lower volatility.

We further classified the detected OOMs into four groups based on the number of nitrate groups they possessed, including non-nitrogen (0N-) OOMs, 1N-OOMs, 2N-OOMs, and 3N-OOMs. Their average fractional contributions to total OOM concentrations as well as the carbon number (nC) distributions are shown in Figure 1. We found 1N-OOMs dominated the total OOM concentration with an average fraction of 50%, followed by 2N-OOMs (26%), demonstrating the dominance of N-containing OOMs among total OOMs. The 3N-OOMs only took up a small fraction (4%) of total OOMs and the rest 20% was 0N-OOMs.

More interestingly, we found 1N-OOMs prevailed among the OOMs with nC⩽10, yet 2N-OOMs dominated the $C_{>10}$ OOMs (41.8-84.2%) and its fraction increased stepwise with the increase of nC (Figure 1b). This is likely because more carbon atoms in the molecular skeleton can potentially provide more active sites for multi-step oxidation, followed by NO termination. Our observation suggests the increased importance of multi-step bimolecular oxidation in the formation of 2N-OOMs with nC>10, which is also consistent with those reported in recent laboratory studies during the oxidation of aromatic and long chain alkanes with the presence of NO. Furthermore, these 2N-OOMs with nC>10 had an average molecular composition of $C_{12.5}H_{22.7}O_{2.1}(NO_3)_2$. Assuming the nitrogen atoms are only associated with nitrate group ($-ONO_2$), the mean double bond equivalent value (DBE) (Nie et al., 2022; Xu et al., 2021) was 1.15 on

https://doi.org/10.5194/acp-2022-774
Preprint. Discussion started: 17 November 2022


Atmospheric Chemistry and Physics Discussions

the carbon skeleton, suggesting its origination from aliphatic compounds, such as alkanes, alkenes, etc. (Gong et al., 2005; Mentel et al., 2015; Wang and Hildebrandt Ruiz, 2018).

We thus further classified the 2N-OOMs to their possible VOC precursors following a recently developed workflow based on the up-to-date understanding of VOC oxidation as well as PMF results (Nie et al., 2022), *i.e.*, aromatics (2N-OOM_{Aro}), aliphatics (2N-OOM_{Ali}), and monoterpene (2N-OOM_{MT}). Note that we group isoprene 2N-OOMs (2N-OOM_{Iso}) into 2N-OOM_{Ali} as well because of the low concentration of isoprene in cold season. As a result, the average fractions of 2N-OOM_{Aro}, 2N-OOM_{Ali} and 2N-OOM_{MT} among total 2N-OOMs were 16.0%, 64.2% and 15.3%, respectively (Figure 2), suggesting significant contribution of aliphatic compounds to 2N-OOMs formation. Taken together, the increased fraction of 2N-OOMs with the increase of nC and the dominant fraction of 2N-OOM_{Ali} highlight the significant contribution of high-molecular-weight aliphatic precursors (*i.e.*, intermediate volatility or semi-volatile organic compounds, I/SVOCs) to high-molecular-weight 2N-OOM formation, which were potentially important SOA material. We thus focus our attention on the formation of 2N-OOMs in the following sections.

3.2 2N-OOM formation in PM episodes

To investigate the formation mechanisms and factors that may affect the 2N-OOM formation, one clean day (4^{th}-5^{th} November) and one polluted day (7^{th}-8^{th} November) based on the pollution levels, *i.e.*, $PM_{2.5}$ concentrations, were selected for further analysis. Since OOM formation is directly mediated by photochemistry or nighttime chemistry, the clean and polluted cases were thus split into one clean daytime case (CL_{day}), one clean nighttime case (CL_{night}), one polluted daytime case (PL_{day}) and one polluted nighttime case (PL_{night}). Detailed information on durations, pollution levels, meteorological conditions and 2N-OOM concentrations during these four cases were summarized in Table 1.

During the whole campaign, the concentrations of 2N-OOMs ranged from 1.1×10^6 to 42.0×10^6 molecule cm^{-3} as shown in Figure 2. We found the concentrations of 2N-OOMs in the polluted cases were 1.7-2.7 times higher than those in clean cases (Table 1). Among the 2N-OOMs, 2N-OOM_{Ali} occupied the largest fractions, which were even higher in polluted cases (66-66%) than those in clean cases (56-61%,

https://doi.org/10.5194/acp-2022-774
Preprint. Discussion started: 17 November 2022


Atmospheric Chemistry and Physics Discussions

Figure 2). Especially for the 2N-OOM_{Ali} with nC>10, its concentration in polluted cases increased by a factor of 2.3-4.8 compared to the clean cases (Figure 3). From PMF analysis, we also identified a factor characterized by a series of 2N-OOM_{Ali} (*i.e.*, $C_nH_{2n-2}O_8N_2$, n=5-11) as the fingerprint molecules (Table S1). This factor tracks the $PM_{2.5}$ concentration well especially during PM episodes (Figure S7), likely due to the availability of adequate aliphatic precursors during pollution episode. Furthermore, 2N-OOM_{Ali} with nC>10 presented both higher concentrations and fractions during daytime than nighttime cases (Figure 3), suggesting that the photochemical formation of 2N-OOM_{Ali} prevailed compared to nighttime formation. To compare CL_{night} and PL_{night}, it was also found that the pollution case would lead enhanced importance of nighttime formation pathways of 2N-OOM_{Ali} with nC>10.

We note that the fraction of 2N-OOM_{Ali} increased during CL_{night} primarily due to the more evident decrease of 2N-OOM_{Aro} (Table 1), whose formation is dominated by photochemistry. On the other hand, the decrease of 2N-OOM_{Aro} concentrations at PL_{night} was not as obvious as those on CL_{night}. Due to the significant increase of 2N-OOM_{Ali} concentration, the fraction of 2N-OOM_{Aro} decreased in pollution cases, but their absolute concentrations only had few changes in the daytime. 2N-OOM_{MT} showed overall higher concentrations during nighttime than those in daytime, suggesting the importance of nighttime chemistry in 2N-OOM_{MT} formation, which will be discussed in later sections.

To summarize, the formation of 2N-OOM_{Ali} were significantly promoted by pollution levels, whereas the 2N-OOM_{Aro} were predominantly affected by photochemical production, whose formation was less sensitive to pollution levels compared to 2N-OOM_{Ali}. In contrast, the concentrations of 2N-OOM_{MT} significantly influenced by pollution levels and seem not solely/almost depend on daytime/nighttime formation pathway. In addition, we note that both daytime photochemistry and nighttime chemistry had profound effects on 2N-OOMs formation under different pollution levels, presumably depending on availability of the precursors as well as the oxidants. We thus focus our attention on the formation of 2N-OOMs during daytime versus nighttime in the following sections.

3.3 Daytime vs. nighttime formation of 2N-OOMs

We thus investigate the effects of photochemistry and nighttime chemistry on the formation of

https://doi.org/10.5194/acp-2022-774
Preprint. Discussion started: 17 November 2022


Atmospheric Chemistry and Physics Discussions

individual 2N-OOMs. While the former is dominated by OH radical oxidation, the latter involves NO_3 radical oxidation as well as reactions with ozone or other oxidants, *e.g.*, halogen. Herein, we use solar radiation as a proxy of photochemical reactivity, and the concentrations of NO_3 radical were estimated assuming that NO_3, NO_2 and N_2O_5 were under fast equilibration in troposphere (Brown and Stutz, 2012). The correlation coefficients (Spearman type) between individual 2N-OOM molecules and solar radiation ($R_{2N\text{-}OOMs\text{-}solar}$) or NO_3 radical ($R_{2N\text{-}OOMs\text{-}NO3}$) derived from different precursors during the whole campaign were shown in Figure 4a.

Both 2N-OOM_{Aro} and 2N-OOM_{Ali} showed stronger correlations with solar radiation over NO_3 radicals, indicating their association with daytime photochemistry since benzene/alkyl benzenes and aliphatic VOCs rapidly react with OH radicals compared to other oxidants, such as NO_3 radicals. This is also supported by the observation that both 2N-OOM_{Aro} and 2N-OOM_{Ali} peaked during noontime (12:00-14:00) as shown in Figure 4b. Similarly, the PMF analysis also distinguished two daytime factors. The daytime factor-1 peaked at around 12:00-14:00 (Table S1) and highly correlated with solar radiation (R=0.57). The fingerprint-molecules of daytime factor-1 are $C_nH_{2n-4}O_{10}N_2$ (n=8-10) with average DBE values of 2 on the carbon skeleton, suggesting the dominance of 2N-OOMs likely formed from aromatic precursors. Since each step of OH oxidation of aromatics followed by RO_2+NO_x termination would increase the nH by one, this factor is likely dominated by 2N-OOMs formed from two steps of OH-initiated oxidation from alkylbenzenes given the carbon numbers ranged from 8 to 10.

The key fingerprint molecule of daytime factor-2 is $C_nH_{2n}O_8N_2$ (n=4-5) (accounting for 30.8% in the factor profile), followed by $C_nH_{2n-2}O_8N_2$ (n=5-6) (accounting for 9.7% in the factor profile), which is likely a result of the decomposition from 2N-OOM_{Ali} with large carbon numbers, according to their DBE values of 0-1 on the carbon skeleton. This aliphatic factor presented even higher correlation with solar radiation (R=0.65), peaking at around 12:00-14:00. Strong daytime peaks together with the good correlations with irradiation suggest the dominance of photochemical oxidation in the formation of 2N-OOM_{Ali}. For 2N-OOM_{Ali}, although it showed strong daytime peak, weak nighttime peak was still observed. This indicates that although daytime formation of 2N-OOM_{Ali} prevails, their nighttime formation still

https://doi.org/10.5194/acp-2022-774
Preprint. Discussion started: 17 November 2022


Atmospheric Chemistry and Physics Discussions

existed. For example, we have obtained a nighttime factor from PMF analysis (nighttime factor-2), whose fingerprint molecules are $C_5H_8O_9N_2$ and $C_nH_{2n}O_7N_2$ (n=5-8). $C_5H_8O_9N_2$ was likely originated from isoprene and $C_nH_{2n}O_7N_2$ were likely from anthropogenic aliphatic precursors.

Besides the nighttime formation of 2N-OOM_{Ali}, nighttime chemistry also dominated the formation of 2N-OOM_{MT}, which showed higher concentrations during the nighttime compared to daytime. This is further supported by the stronger correlation between 2N-OOM_{MT} and NO_3 radicals than solar radiation. Formation of 2N-OOM_{MT} is likely a result of NO_3 radical initiated oxidation. As shown in Figure 5, we have identified a series of 2N-OOM_{MT} molecules with molecular composition of $C_{10}H_{16}O_{7,9,11}N_2$, which showed strong positive correlations with NO_3 radical. The occurrence of propagation reaction from RO_2 to RO was critical to the formation of odd oxygen as proposed in previous chamber studies (Boyd et al., 2015; Claflin and Ziemann, 2018). Therefore, formation of $C_{10}H_{16}O_{7,9,11}N_2$ likely started with the reaction of monoterpene with NO_3 radicals forming a NO_3-$C_{10}H_{16}$ alkyl radical, followed by the formation of organic peroxy radical (RO_2) upon addition of O_2. The RO_2 is then converted to an alkoxy radical (RO) upon reaction with NO. The autoxidation process would then start and stepwise introduce O_2 into the molecule, forming a series of more oxygenated RO_2 radicals, *i.e.*, NO_3-$C_{10}H_{16}(O)(OO)_n$. The NO termination reaction of these RO_2 radicals would finally result in ONs with chemical composition of NO_3-$C_{10}H_{16}(O)(OO)_nO(NO)O$ (n=0, 1, 2).

On the other hand, the reaction rate between monoterpenes (i.e., alpha-pinene, beta-pinene and limonene) and NO_3 are about 60,000-140,000 times faster than that between monoterpenes and O_3 at 293K (MCMv3.1), but the averaged nighttime concentrations of O_3 (22.8 ppb) was only about 18,000 times higher than that of NO_3 (1.3 ppt). Therefore, NO_3-initiated oxidation process posed significant impacts on 2N-OOM_{MT} formation during nighttime. The 2N-OOM_{MT} resulted from NO_3 oxidation is also resolved as a nighttime factor (nighttime factor-1) from PMF analysis, which tracked the NO_3 concentrations very well (Figure S8) and peaked at around 19:00-23:00. Fingerprint molecule of nighttime factor-1 was mainly including $C_{10}H_{16}O_9N_2$ and $C_{10}H_{16}O_8N_2$, which is generated from NO_3-initiated oxidation followed by NO termination and this process will not change the nH of the parent monoterpene molecule.

https://doi.org/10.5194/acp-2022-774
Preprint. Discussion started: 17 November 2022

Atmospheric Chemistry and Physics Discussions

3.4 Oxygenation level of 2N-OOMs

We then calculated the average effective oxygen number (nO_{eff} = nO - 2nN) of 2N-OOMs, which is used to indicate the oxidation state of carbon by excluding the oxygen atoms bonded with nitrogen atoms. Note that calculation of nO_{eff} assumes that the nitrogen atoms are only associated with nitrate group (-ONO_2), which is reasonable after excluding nitrophenol peaks. The average nO_{eff} of 2N-OOMs from different precursors in CL_{day}, CL_{night}, PL_{day} and PL_{night} were shown in Figure 6 and summarized in Table S2. 2N-OOM_{Aro} had the highest nO_{eff} (4.8-5.6), followed by 2N-OOM_{MT} (4.5-4.9) and 2N-OOM_{Ali} were of lowest nO_{eff} (3.9-4.0). Difference in the oxygenation level of different types of OOMs can be attributed to the difference in oxidation mechanisms of the initiation reactions. For example, the OH-initiated oxidation of alkanes, aromatics and monoterpene/alkenes would form a $C_xH_yO_2$ radical, $C_xH_yO_5$ radical and $C_xH_yO_3$ radical, respectively, incorporating different number of oxygen atoms into the original precursor molecules at the first step of oxidation (MCMv3.1). On the other hand, during the multiple-step oxidation in daytime, aromatics could still provide more C=C bonds than other precursors after the initial step which is plausibly capable to further react with OH, O_3 and others oxidants.

Furthermore, we also found that regardless of the pollution level, the nO_{eff} was considerably higher in daytime cases than that in nighttime cases particularly for 2N-OOM_{Aro} and 2N-OOM_{MT}, suggesting a profound effects of photochemistry on the formation of highly oxygenated 2N-OOMs. This is likely because of the high NO_x concentrations during the nighttime (Table 1), which could efficiently suppress the RO_2 radicals from autoxidation reactions forming overall less oxygenated OOM molecules. The effect of NO_x on oxygenation levels would be discussed in a subsequent paragraph. The average nO_{eff} of 2N-OOM_{Ali} in four sub-periods were similar without significant daytime and nighttime difference, ranging from 3.9-4.0. This could be partly explained by the fact that reactions with oxidants such as OH and halogen radicals will similarly result in the addition of oxygen atoms by two for alkanes during the first step of oxidation. Thus, the oxygenation levels of 2N-OOM_{Ali} were supposed to be insensitive to the oxidants in daytime or nighttime.

It is known that NO_x is also critical in determining the fate of RO_2 radical during the oxidation,

https://doi.org/10.5194/acp-2022-774
Preprint. Discussion started: 17 November 2022


Atmospheric Chemistry and Physics Discussions

forming RO radicals or organonitrates. Formation of RO radicals and organonitrates will have opposite effects on the oxidation state of the termination products since the former will significantly increase the oxygenation state of carbon through initiating propagation reactions before termination. We thus explore the effects of NO_x on the average oxygenation levels of 2N-OOMs from different precursors during the whole campaign (Figure 7). Consistent with previous studies in polluted urban environment (Qiao et al., 2021; Yan et al., 2021), the detected 2N-OOMs were also of low oxygenation with nO_{eff} of 3.9-5.4 (25-75% percentile) compared to those measured in forest or in laboratory studies (Berndt et al., 2016; Ehn et al., 2014; Jokinen et al., 2014; Rissanen et al., 2014; Yan et al., 2016). nO_{eff} of 2N-OOM_{Aro} and 2N-OOM_{MT} increased with the decrease of NO_x concentrations. This is likely due to the prevailing of NO_x termination reactions because the maximum autoxidation rate constant of alkylbenzenes with long-chain substituents (e.g., isopropyl-benzene, ethyl-benzene) and monoterpene are comparable to the bimolecular reaction rate between RO_2 and NO (Bianchi et al., 2019). The oxygenation levels of 2N-OOM_{Ali} appears to be insensitive to the pollution levels and NO_x concentrations, which should be further investigated in future studies.

4 Conclusion

We report the unambiguous identification of 2N-OOMs as well as other OOMs using an ultra-high-resolution orbitrap coupled with a nitrate inlet. We found that OOMs distributed in a wide range of carbon numbers (nC = 4 - 16), among which the 2N-OOMs occupied a considerable fraction (26%) of the total observed OOMs. During the whole campaign, the 2N-OOM concentrations ranged from 1.1×10^6 to 42.0×10^6 molecule cm^{-3} and concentrated in the nC range of 5 to 10 with high molecular weight ($m/z >$ 350 Th), suggesting their low volatilities and thus potentially high contribution to local SOA formation.

Aliphatic, aromatics, and monoterpenes were plausible precursors of 2N-OOMs with a fraction of 64.2%, 16% and 15.4%, respectively. The 2N-OOM_{Ali} was found to be the most abundant 2N-OOMs and its fraction even increased in the polluted day with enhanced proportion of ones with nC>10, probably due to the high concentrations of aliphatic precursors accompanied with PM episodes. Significant contribution of long-chain aliphatic compounds (nC > 10) to 2N-OOM formation is also supported by the

https://doi.org/10.5194/acp-2022-774
Preprint. Discussion started: 17 November 2022

Atmospheric Chemistry and Physics Discussions

observation that 2N-OOM fraction increased with the increase of nC and they are of low DBE values, likely through multistep bimolecular oxidation. 2N-OOM_{Ali} and 2N-OOM_{Aro} mainly peaked in daytime and showed stronger correlations with solar radiation over NO_3 radicals, indicating their association with daytime photochemistry since benzene/alkyl benzenes and aliphatic hydrocarbons rapidly react with OH radicals compared with other oxidants, such as NO_3 radicals. In contrast, 2N-OOM_{MT} prevailed during nighttime and also showed higher correlations with estimated NO_3 radical concentrations than solar radiation, suggesting that NO_3-initiated oxidation of monoterpene dominated the formation of 2N-OOM_{MT} during nighttime even under the polluted urban environment, *i.e.*, high NO_x. In terms of oxygenation levels, we found that 2N-OOM_{Aro} had highest averaged nO_{eff} followed by 2N-OOM_{MT}. Daytime photochemistry and low NO_x concentrations had profound effects on the formation of more oxygenated 2N-OOMs. 2N-OOM_{Ali} had the lowest nO_{eff} and had negligible changes under different pollution levels. These results demonstrate the preference of 2N-OOM formation and the influencing factors in a Chinese megacity involving various VOC precursors (biogenic VOCs such as monoterpene and anthropogenic VOCs such as aromatics, aliphatic hydrocarbons) and various atmospheric oxidants (such as OH radical and NO_3 radicals), and highlight the influence of PM episode.

Code/Data availability

Data presented in this paper are available upon request to the corresponding author.

Author contributions

CH designed this study. YL, YM, DDH, SL, SJ, and YG conducted the field campaign. YL analyzed data with contributions from CH and all the other co-authors. YL wrote the manuscript with contributions from all the other co-authors.

Competing interests

The authors declare that they have no conflict of interest.

Acknowledgement

This study was financially supported by the Funded by the National Key R&D Program of China (2022YFC3700205), and China Postdoctoral Science Foundation (2022T150427).

https://doi.org/10.5194/acp-2022-774
Preprint. Discussion started: 17 November 2022

Atmospheric Chemistry and Physics Discussions

Reference

Atkinson, R. and Arey, J.: Atmospheric Degradation of Volatile Organic Compounds, Chem. Rev., 103(3), 4605–4638, doi:10.1021/cr0206420, 2003.

Berndt, T., Richters, S., Jokinen, T., Hyttinen, N., Kurtén, T., Otkjær, R. V., Kjaergaard, H. G., Stratmann, F., Herrmann, H., Sipilä, M., Kulmala, M. and Ehn, M.: Hydroxyl radical-induced formation of highly oxidized organic compounds, Nat. Commun., 7(13677), doi:10.1038/ncomms13677, 2016.

Berndt, T., Scholz, W., Mentler, B., Fischer, L., Herrmann, H., Kulmala, M. and Hansel, A.: Accretion Product Formation from Self- and Cross-Reactions of RO2 Radicals in the Atmosphere, Angew. Chemie - Int. Ed., 57(14), 3820–3824, doi:10.1002/anie.201710989, 2018.

Bianchi, F., Kurtén, T., Riva, M., Mohr, C., Rissanen, M. P., Roldin, P., Berndt, T., Crounse, J. D., Wennberg, P. O., Mentel, T. F., Wildt, J., Junninen, H., Jokinen, T., Kulmala, M., Worsnop, D. R., Thornton, J. A., Donahue, N., Kjaergaard, H. G. and Ehn, M.: Highly Oxygenated Molecules (HOM) from Gas-Phase Autoxidation Involving Organic Peroxy Radicals: A Key Contributor to Atmospheric Aerosol, Chem. Rev., 119, 3472–3509, doi:10.1021/acs.chemrev.8b00395, 2019.

Boyd, C. M., Sanchez, J., Xu, L., Eugene, A. J., Nah, T., Tuet, W. Y., Guzman, M. I. and Ng, N. L.: Secondary organic aerosol formation from the β-pinene+NO3 system: Effect of humidity and peroxy radical fate, Atmos. Chem. Phys., 15(13), 7497–7522, doi:10.5194/acp-15-7497-2015, 2015.

Brown, S. S. and Stutz, J.: Nighttime radical observations and chemistry, Chem. Soc. Rev., 41, 6405–6447, doi:10.1039/c2cs35181a, 2012.

Cai, R., Li, Y., Clément, Y., Li, D., Dubois, C., Fabre, M., Besson, L., Perrier, S., George, C., Ehn, M., Huang, C., Yi, P., Ma, Y. and Riva, M.: Orbitool: A software tool for analyzing online Orbitrap mass spectrometry data, Atmos. Meas. Tech., 14, 2377–2387, doi:10.5194/amt-2020-267, 2020.

Canonaco, F., Crippa, M., Slowik, J. G., Baltensperger, U. and Prévôt, A. S. H. H.: SoFi, an IGOR-based interface for the efficient use of the generalized multilinear engine (ME-2) for the source apportionment: ME-2 application to aerosol mass spectrometer data, Atmos. Meas. Tech., 6(12), 3649–3661, doi:10.5194/amt-6-3649-2013, 2013.

https://doi.org/10.5194/acp-2022-774
Preprint. Discussion started: 17 November 2022


Atmospheric Chemistry and Physics Discussions

369 Claflin, M. S. and Ziemann, P. J.: Identification and Quantitation of Aerosol Products of the Reaction of
370 β-Pinene with NO3 Radicals and Implications for Gas- and Particle-Phase Reaction Mechanisms, J.
371 Phys. Chem. A, 122(14), 3640–3652, doi:10.1021/acs.jpca.8b00692, 2018.
372 Ditto, J. C., Joo, T., Slade, J. H., Shepson, P. B., Ng, N. L. and Gentner, D. R.: Nontargeted Tandem Mass
373 Spectrometry Analysis Reveals Diversity and Variability in Aerosol Functional Groups across
374 Multiple Sites, Seasons, and Times of Day, Environ. Sci. Technol. Lett., 7(2), 60–69,
375 doi:10.1021/acs.estlett.9b00702, 2020.
376 Donahue, N. M., Robinson, A. L. and Pandis, S. N.: Atmospheric organic particulate matter: From smoke
377 to secondary organic aerosol, Atmos. Environ., 43(1), 94–106, doi:10.1016/j.atmosenv.2008.09.055,
378 2009.
379 Donahue, N. M., Epstein, S. A., Pandis, S. N. and Robinson, A. L.: A two-dimensional volatility basis set:
380 1. organic-aerosol mixing thermodynamics, Atmos. Chem. Phys., 11(7), 3303–3318,
381 doi:10.5194/acp-11-3303-2011, 2011.
382 Donahue, N. M., Kroll, J. H., Pandis, S. N. and Robinson, A. L.: A two-dimensional volatility basis set-
383 Part 2: Diagnostics of organic-aerosol evolution, Atmos. Chem. Phys., 12(2), 615–634,
384 doi:10.5194/acp-12-615-2012, 2012.
385 Ehn, M., Thornton, J. A., Kleist, E., Sipilä, M., Junninen, H., Pullinen, I., Springer, M., Rubach, F.,
386 Tillmann, R., Lee, B., Lopez-Hilfiker, F., Andres, S., Acir, I.-H. H., Rissanen, M., Jokinen, T.,
387 Schobesberger, S., Kangasluoma, J., Kontkanen, J., Nieminen, T., Kurtén, T., Nielsen, L. B.,
388 Jørgensen, S., Kjaergaard, H. G., Canagaratna, M., Maso, M. D., Berndt, T., Petäjä, T., Wahner, A.,
389 Kerminen, V.-M. M., Kulmala, M., Worsnop, D. R., Wildt, J. and Mentel, T. F.: A large source of
390 low-volatility secondary organic aerosol, Nature, 506(7489), 476–479, doi:10.1038/nature13032,
391 2014.
392 Garmash, O., Rissanen, M. P., Pullinen, I., Schmitt, S., Kausiala, O., Tillmann, R., Zhao, D., Percival, C.,
393 Bannan, T. J., Priestley, M., Hallquist, A. M., Kleist, E., Kiendler-Scharr, A., Hallquist, M., Berndt,
394 T., McFiggans, G., Wildt, J., Mentel, T. F. and Ehn, M.: Multi-generation OH oxidation as a source

https://doi.org/10.5194/acp-2022-774
Preprint. Discussion started: 17 November 2022


Atmospheric Chemistry and Physics Discussions

for highly oxygenated organic molecules from aromatics, Atmos. Chem. Phys., 20(1), 515–537, doi:10.5194/acp-20-515-2020, 2020.

Gong, H., Matsunaga, A. and Ziemann, P. J.: Products and mechanism of secondary organic aerosol formation from reactions of linear alkenes with NO3 Radicals, J. Phys. Chem. A, 109(19), 4312–4324, doi:10.1021/jp058024l, 2005.

Hallquist, M., Wenger, J. C., Baltensperger, U., Rudich, Y., Simpson, D., Claeys, M., Dommen, J., Donahue, N. M., George, C., Goldstein, A. H., Hamilton, J. F., Herrmann, H., Hoffmann, T., Iinuma, Y., Jang, M., Jenkin, M. E., Jimenez, J. L., Kiendler-Scharr, A., Maenhaut, W., McFiggans, G., Mentel, T. F., Monod, A., Prévôt, A. S. H., Seinfeld, J. H., Surratt, J. D., Szmigielski, R. and Wildt, J.: The formation, properties and impact of secondary organic aerosol: Current and emerging issues, Atmos. Chem. Phys., 9(14), 5155–5236, doi:10.5194/acp-9-5155-2009, 2009.

Heinritzi, M., Simon, M., Steiner, G., Wagner, A. C., K??rten, A., Hansel, A. and Curtius, J.: Characterization of the mass-dependent transmission efficiency of a CIMS, Atmos. Meas. Tech., 9(4), 1449–1460, doi:10.5194/amt-9-1449-2016, 2016.

Hyttinen, N., Kupiainen-Määtta, O., Rissanen, M. P., Muuronen, M., Ehn, M. and Kurtén, T.: Modeling the Charging of Highly Oxidized Cyclohexene Ozonolysis Products Using Nitrate-Based Chemical Ionization, J. Phys. Chem. A, 119(24), 6339–6345, doi:10.1021/acs.jpca.5b01818, 2015.

Hyttinen, N., Otkjær, R. V., Iyer, S., Kjaergaard, H. G., Rissanen, M. P., Wennberg, P. O. and Kurtén, T.: Computational Comparison of Different Reagent Ions in the Chemical Ionization of Oxidized Multifunctional Compounds, J. Phys. Chem. A, 122(1), 269–279, doi:10.1021/acs.jpca.7b10015, 2018.

Jimenez, J. L., Canagaratna, M. R., Donahue, N. M., Prevot, A. S. H. H., Zhang, Q., Kroll, J. H., DeCarlo, P. F., Allan, J. D., Coe, H., Ng, N. L., Aiken, A. C., Docherty, K. S., Ulbrich, I. M., Grieshop, A. P., Robinson, A. L., Duplissy, J., Smith, J. D., Wilson, K. R., Lanz, V. A., Hueglin, C., Sun, Y. L., Tian, J., Laaksonen, A., Raatikainen, T., Rautiainen, J., Vaattovaara, P., Ehn, M., Kulmala, M., Tomlinson, J. M., Collins, D. R., Cubison, M. J., Dunlea, J., Huffman, J. A., Onasch, T. B., Alfarra, M. R.,

https://doi.org/10.5194/acp-2022-774
Preprint. Discussion started: 17 November 2022


Atmospheric Chemistry and Physics Discussions

421 Williams, P. I., Bower, K., Kondo, Y., Schneider, J., Drewnick, F., Borrmann, S., Weimer, S.,
422 Demerjian, K., Salcedo, D., Cottrell, L., Griffin, R., Takami, A., Miyoshi, T., Hatakeyama, S.,
423 Shimono, A., Sun, J. Y., Zhang, Y. M., Dzepina, K., Kimmel, J. R., Sueper, D., Jayne, J. T., Herndon,
424 S. C., Trimborn, A. M., Williams, L. R., Wood, E. C., Middlebrook, A. M., Kolb, C. E., Baltensperger,
425 U., Worsnop, D. R., Dunlea, E. J., Huffman, J. A., Onasch, T. B., Alfarra, M. R., Williams, P. I.,
426 Bower, K., Kondo, Y., Schneider, J., Drewnick, F., Borrmann, S., Weimer, S., Demerjian, K.,
427 Salcedo, D., Cottrell, L., Griffin, R., Takami, A., Miyoshi, T., Hatakeyama, S., Shimono, A., Sun, J.
428 Y., Zhang, Y. M., Dzepina, K., Kimmel, J. R., Sueper, D., Jayne, J. T., Herndon, S. C., Trimborn, A.
429 M., Williams, L. R., Wood, E. C., Middlebrook, A. M., Kolb, C. E., Baltensperger, U. and Worsnop,
430 D. R.: Evolution of Organic Aerosols in the Atmosphere, Science (80-.)., 326(5959), 1525–1529,
431 doi:10.1126/science.1180353, 2009.
432 Jokinen, T., Sipilä, M., Richters, S., Kerminen, V. M., Paasonen, P., Stratmann, F., Worsnop, D., Kulmala,
433 M., Ehn, M., Herrmann, H. and Berndt, T.: Rapid autoxidation forms highly oxidized RO2 radicals
434 in the atmosphere, Angew. Chemie Int. Ed., 53, 14596–14600, doi:10.1002/anie.201408566, 2014.
435 Jokinen, T., Berndt, T., Makkonen, R., Kerminen, V.-M., Junninen, H., Paasonen, P., Stratmann, F.,
436 Herrmann, H., Guenther, A. B., Worsnop, D. R., Kulmala, M., Ehn, M. and Sipilä, M.: Production
437 of extremely low volatile organic compounds from biogenic emissions: Measured yields and
438 atmospheric implications, Proc. Natl. Acad. Sci., 112(23), 7123–7128,
439 doi:10.1073/pnas.1423977112, 2015.
440 Junninen, H., Ehn, M., Petäjä, Luosujärvi, L., Kotiaho, T., Kostiainen, R., Rohner, U., Gonin, M., Fuhrer,
441 K., Kulmala, M. and Worsnop, D. R.: A high-resolution mass spectrometer to measure atmospheric
442 ion composition, Atmos. Meas. Tech., 3(4), 1039–1053, doi:10.5194/amt-3-1039-2010, 2010.
443 Kiendler-Scharr, A., Mensah, A. A., Friese, E., Topping, D., Nemitz, E., Prevot, A. S. H., Äijälä, M.,
444 Allan, J., Canonaco, F., Canagaratna, M., Carbone, S., Crippa, M., Dall Osto, M., Day, D. A., De
445 Carlo, P., Di Marco, C. F., Elbern, H., Eriksson, A., Freney, E., Hao, L., Herrmann, H., Hildebrandt,
446 L., Hillamo, R., Jimenez, J. L., Laaksonen, A., McFiggans, G., Mohr, C., O'Dowd, C., Otjes, R.,

https://doi.org/10.5194/acp-2022-774
Preprint. Discussion started: 17 November 2022


Atmospheric Chemistry and Physics Discussions

447 Ovadnevaite, J., Pandis, S. N., Poulain, L., Schlag, P., Sellegri, K., Swietlicki, E., Tiitta, P.,
448 Vermeulen, A., Wahner, A., Worsnop, D. and Wu, H. C.: Ubiquity of organic nitrates from nighttime
449 chemistry in the European submicron aerosol, Geophys. Res. Lett., 43(14), 7735–7744,
450 doi:10.1002/2016GL069239, 2016.
451 Lee, B. H., Mohr, C., Lopez-Hilfiker, F. D., Lutz, A., Hallquist, M., Lee, L., Romer, P., Cohen, R. C.,
452 Iyer, S., Kurtén, T., Hu, W., Day, D. A., Campuzano-Jost, P., Jimenez, J. L., Xu, L., Ng, N. L., Guo,
453 H., Weber, R. J., Wild, R. J., Brown, S. S., Koss, A., De Gouw, J., Olson, K., Goldstein, A. H., Seco,
454 R., Kim, S., McAvey, K., Shepson, P. B., Starn, T., Baumann, K., Edgerton, E. S., Liu, J., Shilling,
455 J. E., Miller, D. O., Brune, W., Schobesberger, S., D'Ambro, E. L. and Thornton, J. A.: Highly
456 functionalized organic nitrates in the southeast United States: Contribution to secondary organic
457 aerosol and reactive nitrogen budgets, Proc. Natl. Acad. Sci. U. S. A., 113(6), 1516–1521,
458 doi:10.1073/pnas.1508108113, 2016.
459 Liebmann, J., Sobanski, N., Schuladen, J., Karu, E., Hellén, H., Hakola, H., Zha, Q., Ehn, M., Riva, M.,
460 Williams, J., Fischer, H., Lelieveld, J. and Crowley, J. N.: Alkyl nitrates in the boreal forest:
461 Formation via the NO3, OH and O3 induced oxidation of BVOCs and ambient lifetimes, Atmos.
462 Chem. Phys. Discuss., (3), 1–23, doi:10.5194/acp-2019-463, 2019.
463 Lin, C., Huang, R. J., Duan, J., Zhong, H. and Xu, W.: Primary and Secondary Organic Nitrate in
464 Northwest China: A Case Study, Environ. Sci. Technol. Lett., 8(11), 947–953,
465 doi:10.1021/acs.estlett.1c00692, 2021.
466 Mentel, T. F., Springer, M., Ehn, M., Kleist, E., Pullinen, I., Kurtén, T., Rissanen, M., Wahner, A. and
467 Wildt, J.: Formation of highly oxidized multifunctional compounds: autoxidation of peroxy radicals
468 formed in the ozonolysis of alkenes-deduced from structure–product relationships, Atmos. Chem.
469 Phys. Discuss., 15(2), 2791–2851, doi:10.5194/acpd-15-2791-2015, 2015.
470 Nie, W., Yan, C., Huang, D. D., Wang, Z., Liu, Y., Qiao, X., Guo, Y., Tian, L., Zheng, P., Xu, Z., Li, Y.,
471 Xu, Z., Qi, X., Sun, P., Wang, J., Zheng, F., Li, X., Yin, R., Dallenbach, K. R., Bianchi, F., Petäjä,
472 T., Zhang, Y., Wang, M., Schervish, M., Wang, S., Qiao, L., Wang, Q., Zhou, M., Wang, H., Yu, C.,

https://doi.org/10.5194/acp-2022-774
Preprint. Discussion started: 17 November 2022


Atmospheric Chemistry and Physics Discussions

473 Yao, D., Guo, H., Ye, P., Lee, S., Li, Y. J., Liu, Y., Chi, X., Kerminen, V.-M., Ehn, M., Donahue, N.
474 M., Wang, T., Huang, C., Kulmala, M., Worsnop, D., Jiang, J. and Ding, A.: Secondary organic
475 aerosol formed by condensing anthropogenic vapours over China's megacities, Nat. Geosci., 15,
476 255–261, doi:10.1038/s41561-022-00922-5, 2022.
477 Pye, H. O. T., D'Ambro, E. L., Lee, B. H., Schobesberger, S., Takeuchi, M., Zhao, Y., Lopez-Hilfiker, F.,
478 Liu, J., Shilling, J. E., Xing, J., Mathur, R., Middlebrook, A. M., Liao, J., Welti, A., Graus, M.,
479 Warneke, C., de Gouw, J. A., Holloway, J. S., Ryerson, T. B., Pollack, I. B. and Thornton, J. A.:
480 Anthropogenic enhancements to production of highly oxygenated molecules from autoxidation, Proc.
481 Natl. Acad. Sci. U. S. A., 116(14), 6641–6646, doi:10.1073/pnas.1810774116, 2019.
482 Qiao, X., Yan, C., Li, X., Guo, Y., Yin, R., Deng, C., Li, C., Nie, W., Wang, M., Cai, R., Huang, D., Wang,
483 Z., Yao, L., Worsnop, D. R., Bianchi, F., Liu, Y., Donahue, N. M., Kulmala, M. and Jiang, J.:
484 Contribution of Atmospheric Oxygenated Organic Compounds to Particle Growth in an Urban
485 Environment, Environ. Sci. Technol., doi:10.1021/acs.est.1c02095, 2021.
486 Rissanen, M. P., Kurtén, T., Sipilä, M., Thornton, J. A., Kangasluoma, J., Sarnela, N., Junninen, H.,
487 Jørgensen, S., Schallhart, S., Kajos, M. K., Taipale, R., Springer, M., Mentel, T. F., Ruuskanen, T.,
488 Petäjä, T., Worsnop, D. R., Kjaergaard, H. G. and Ehn, M.: The formation of highly oxidized
489 multifunctional products in the ozonolysis of cyclohexene, J. Am. Chem. Soc., 136(44), 15596–
490 15606, doi:10.1021/ja507146s, 2014.
491 Riva, M.: Multiphase Chemistry of Highly Oxidized Molecules: The Case of Organic Hydroperoxides,
492 Chem, 1(4), 526–528, doi:10.1016/j.chempr.2016.09.015, 2016.
493 Riva, M., Ehn, M., Li, D., Tomaz, S., Bourgain, F., Perrier, S. and George, C.: CI-Orbitrap: An Analytical
494 Instrument to Study Atmospheric Reactive Organic Species, Anal. Chem., 91, 9419–9423,
495 doi:10.1021/acs.analchem.9b02093, 2019a.
496 Riva, M., Rantala, P., Krechmer, J. E., Peräkylä, O., Zhang, Y., Heikkinen, L., Garmash, O., Yan, C.,
497 Kulmala, M., Worsnop, D. and Ehn, M.: Evaluating the performance of five different chemical
498 ionization techniques for detecting gaseous oxygenated organic species, Atmos. Meas. Tech., 12,

https://doi.org/10.5194/acp-2022-774
Preprint. Discussion started: 17 November 2022


Atmospheric Chemistry and Physics Discussions

2403–2421, doi:10.5194/amt-2018-407, 2019b.

Rollins, A. W., Pusede, S., Wooldridge, P., Min, K. E., Gentner, D. R., Goldstein, A. H., Liu, S., Day, D. A., Russell, L. M., Rubitschun, C. L., Surratt, J. D. and Cohen, R. C.: Gas/particle partitioning of total alkyl nitrates observed with TD-LIF in Bakersfield, J. Geophys. Res. Atmos., 118(12), 6651–6662, doi:10.1002/jgrd.50522, 2013.

Schervish, M. and Donahue, N. M.: Peroxy radical chemistry and the volatility basis set, Atmos. Chem. Phys., 20(2), 1183–1199, doi:10.5194/acp-20-1183-2020, 2020.

Wang, D. S. and Hildebrandt Ruiz, L.: Chlorine-initiated oxidation of n-alkanes under high NOx conditions: Insights into secondary organic aerosol composition and volatility using a FIGAERO-CIMS, Atmos. Chem. Phys. Discuss., (x), 1–26, doi:10.5194/acp-2018-443, 2018.

Wang, Y., Mehra, A., Krechmer, J., Yang, G., Hu, X., Lu, Y., Lambe, A., Canagaratna, M., Chen, J., Worsnop, D., Coe, H. and Wang, L.: Oxygenated products formed from OH-initiated reactions of trimethylbenzene: Autoxidation and accretion, Atmos. Chem. Phys., 20, 9563–9579, doi:10.5194/acp-2020-165, 2020.

Xu, L., Suresh, S., Guo, H., Weber, R. J. and Ng, N. L.: Aerosol characterization over the southeastern United States using high-resolution aerosol mass spectrometry: Spatial and seasonal variation of aerosol composition and sources with a focus on organic nitrates, Atmos. Chem. Phys., 15(13), 7307–7336, doi:10.5194/acp-15-7307-2015, 2015.

Xu, Z. N., Nie, W., Liu, Y. L., Sun, P., Huang, D. D., Yan, C., Krechmer, J., Ye, P. L., Xu, Z., Qi, X. M., Zhu, C. J., Li, Y. Y., Wang, T. Y., Wang, L., Huang, X., Tang, R. Z., Guo, S., Xiu, G. L., Fu, Q. Y., Worsnop, D., Chi, X. G. and Ding, A. J.: Multifunctional Products of Isoprene Oxidation in Polluted Atmosphere and Their Contribution to SOA, Geophys. Res. Lett., 48(1), 1–10, doi:10.1029/2020GL089276, 2021.

Yan, C., Nie, W., Äijälä, M., Rissanen, M. P., Canagaratna, M. R., Massoli, P., Junninen, H., Jokinen, T., Sarnela, N., Häme, S. A. K., Schobesberger, S., Canonaco, F., Yao, L., Prévôt, A. S. H., Petäjä, T., Kulmala, M., Sipilä, M., Worsnop, D. R. and Ehn, M.: Source characterization of highly oxidized

https://doi.org/10.5194/acp-2022-774
Preprint. Discussion started: 17 November 2022


Atmospheric Chemistry and Physics Discussions

multifunctional compounds in a boreal forest environment using positive matrix factorization, Atmos. Chem. Phys., 16, 12715–12731, doi:10.5194/acp-16-12715-2016, 2016.

Yan, C., Yin, R., Lu, Y., Dada, L., Yang, D., Fu, Y., Kontkanen, J., Deng, C., Garmash, O., Ruan, J., Baalbaki, R., Schervish, M., Cai, R., Bloss, M., Chan, T., Chen, T., Chen, Q., Chen, X., Chen, Y., Chu, B., Dällenbach, K., Foreback, B., He, X., Heikkinen, L., Jokinen, T., Junninen, H., Kangasluoma, J., Kokkonen, T., Kurppa, M., Lehtipalo, K., Li, H., Li, H., Li, X., Liu, Y., Ma, Q., Paasonen, P., Rantala, P., Pileci, R. E., Rusanen, A., Sarnela, N., Simonen, P., Wang, S., Wang, W., Wang, Y., Xue, M., Yang, G., Yao, L., Zhou, Y., Kujansuu, J., Petäjä, T., Nie, W., Ma, Y., Ge, M., He, H., Donahue, N. M., Worsnop, D. R., Veli-Matti Kerminen, Wang, L., Liu, Y., Zheng, J., Kulmala, M., Jiang, J. and Bianchi, F.: The Synergistic Role of Sulfuric Acid, Bases, and Oxidized Organics Governing New-Particle Formation in Beijing, Geophys. Res. Lett., 48, 2020GL091944, doi:10.1029/2020gl091944, 2021.

Ye, C., Yuan, B., Lin, Y., Wang, Z., Hu, W., Li, T., Chen, W., Wu, C., Wang, C., Huang, S., Qi, J., Wang, B., Wang, C., Song, W., Wang, X., Zheng, E., Krechmer, J. E., Ye, P., Zhang, Z., Wang, X., Worsnop, D. R. and Shao, M.: Chemical characterization of oxygenated organic compounds in the gas phase and particle phase using iodide CIMS with FIGAERO in urban air, Atmos. Chem. Phys., 21(11), 8455–8478, doi:10.5194/acp-21-8455-2021, 2021.

Yu, K., Zhu, Q., Du, K. and Huan, X. F.: Characterization of nighttime formation of particulate organic nitrates based on high-resolution aerosol mass spectrometry in an urban atmosphere in China, Atmos. Chem. Phys., 19(7), 5235–5249, doi:10.5194/acp-19-5235-2019, 2019.

Zhang, Y., Li, D., Ma, Y., Dubois, C., Wang, X., Perrier, S., Chen, H., Wang, H., Jing, S., Lu, Y., Lou, S., Yan, C., Nie, W., Chen, J., Huang, C., George, C. and Riva, M.: Field Detection of Highly Oxygenated Organic Molecules in Shanghai by Chemical Ionization–Orbitrap, Environ. Sci. Technol., doi:10.1021/acs.est.1c08346, 2022.

Zhao, Y., Thornton, J. A. and Pye, H. O. T.: Quantitative constraints on autoxidation and dimer formation from direct probing of monoterpene-derived peroxy radical chemistry, Proc. Natl. Acad. Sci. U. S.

https://doi.org/10.5194/acp-2022-774
Preprint. Discussion started: 17 November 2022

Atmospheric Chemistry and Physics Discussions

551 A., 115(48), 12142–12147, doi:10.1073/pnas.1812147115, 2018.

552

Open Access
Atmospheric Chemistry and Physics Discussions

Table 1 Summary of the four cases including the meteorological conditions and concentrations of trace gases and 2N-OOMs

Case	Time	$\overline{PM_{2.5}}$ (μg m^{-3})	$\overline{Solar}$ (W m^{-2})	$\bar{T}$ (°C)	$\overline{RH}$ (%)	$\overline{[O_3]}$ (ppb)	$\overline{[NO]}$ (ppb)	$\overline{[NO_2]}$ (ppb)	$\overline{[NO_3]}$ (ppt)	$\overline{[2N-OOM_{Aro}]}$ (×10^6 cm^{-3})	$\overline{[2N-OOM_{Ali}]}$ (×10^6 cm^{-3})	$\overline{[2N-OOM_{MT}]}$ (×10^6 cm^{-3})	$\overline{[2N-OOM_{Total}]}$ (×10^6 cm^{-3})
CL_{day}	Nov. 4th 12:00 - 14:00	7.5	635.6	18.9	35.2	41.9	3.2	8.2	0.1	6.3	11.7	2.3	20.8
CL_{night}	Nov. 4th 23:00 - Nov. 5th 01:00	9.5	2.4	13.0	64.1	8.0	2.9	40.5	0.2	1.3	6.0	2.3	9.8
PL_{day}	Nov. 7th 12:00 - 14:00	44.0	384.5	23.9	30.5	73.9	2.2	20.6	0.3	6.4	23.8	4.3	36.2
PL_{night}	Nov. 7th 23:00 - Nov. 8th 01:00	60.5	2.5	17.8	44.9	27.2	2.1	38.7	6.2	3.1	17.4	5.3	26.5

https://doi.org/10.5194/acp-2022-774
Preprint. Discussion started: 17 November 2022

https://doi.org/10.5194/acp-2022-774
Preprint. Discussion started: 17 November 2022

Atmospheric Chemistry and Physics Discussions

Figure Captions

Figure 1. (a) Average mass spectrum of the detected OOMs during the whole campaign. The pie chart shows the fractions of OOMs with different number of nitrogen and carbon atoms; (b) The fractions of 0N-OOMs, 1N-OOMs, 2N-OOMs and 3N-OOMs among total OOMs as a function of carbon number (nC).

Figure 2. The timeseries of 2N-OOMs originated from different precursors. Four sub-periods were selected to further investigate the fractional distribution of different type of OOM molecules as shown in the pie chart, including a clean daytime case (12:00 to 14:00 on November 4th, $PM_{2.5}$=7.5 μg m^{-3}, CL_{day}), a clean nighttime case (23:00 on November 4th to 01:00 on November 5th, $PM_{2.5}$=9.5 μg m^{-3}, CL_{night}), a daytime case in a PM episode (12:00 to 14:00 on November 7th, $PM_{2.5}$=44.0 μg m^{-3}, PL_{day}) and a nighttime case in a PM episode (23:00 on November 7th to 01:00 on November 8th, $PM_{2.5}$=60.5 μg m^{-3}, PL_{night}). The sizes of pie charts are scaled to the total concentrations of 2N-OOMs.

Figure 3. The fractions of $2N\text{-}OOM_{Ali}$ with different carbon numbers in the four cases.

Figure 4. (a) Statistical distribution of the correlation coeffients (Spearman type) between 2N-OOMs and solar radiation ($R_{2N\text{-}OOMs\ -\ solar}$) in red and the correlation coeffients between 2N-OOMs and [NO_3] ($R_{2N\text{-}OOMs\ -\ NO3}$) in blue for 2N-OOMs from different precursors. The horizontal lines are the median values, boxes denote the 25th- and 75th- percentile values, and whiskers represent the 10th- and 90th- percentile values. (b) The diel patterns of 2N-OOMs from different precursors.

Figure 5. Scatter plot of $R_{2N\text{-}OOMs\ -\ NO3}$ against $R_{2N\text{-}OOMs\ -\ solar}$ for specific 2N-OOM species.

Figure 6. The nO_{eff} of 2N-OOMs derived from different precursors in the four cases, the error bars represent the standard deviations.

Figure 7. Effective oxygen number (nO_{eff}) of 2N-OOMs against NO_x concentration, the lines represent the median value while the shadows denote the 25th- and 75th- percentile values.

https://doi.org/10.5194/acp-2022-774
Preprint. Discussion started: 17 November 2022

Atmospheric Chemistry and Physics Discussions

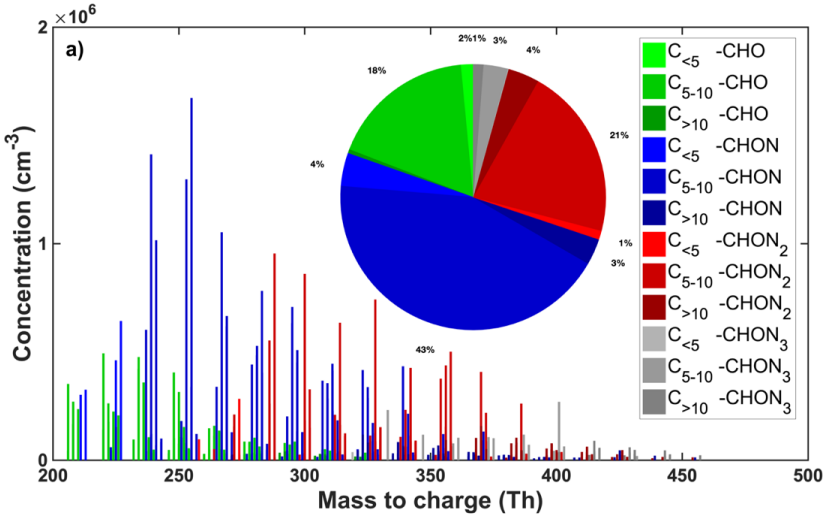

Figure 1a

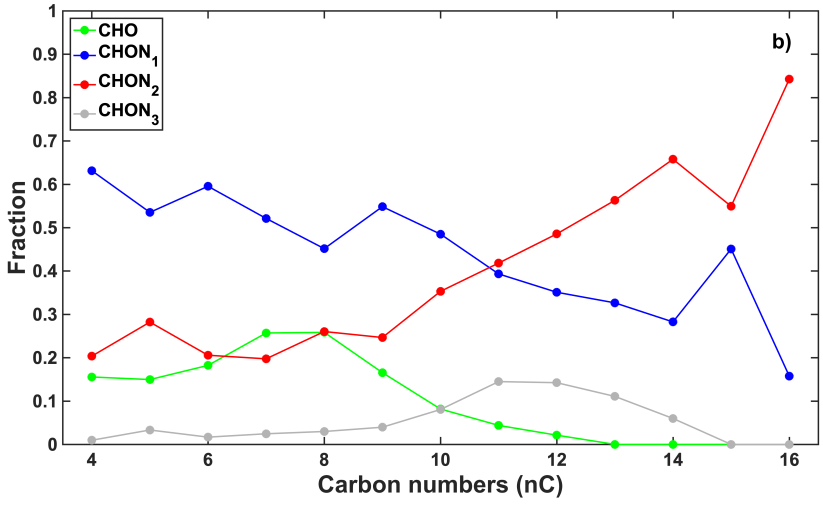

Figure 1b

https://doi.org/10.5194/acp-2022-774
Preprint. Discussion started: 17 November 2022

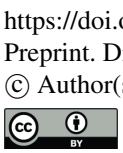

Atmospheric Chemistry and Physics Discussions

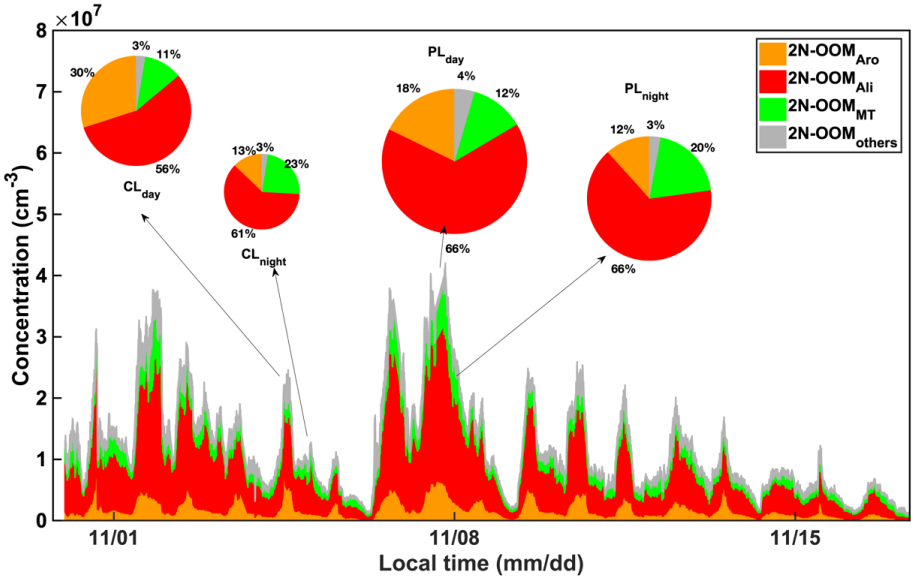

Figure 2

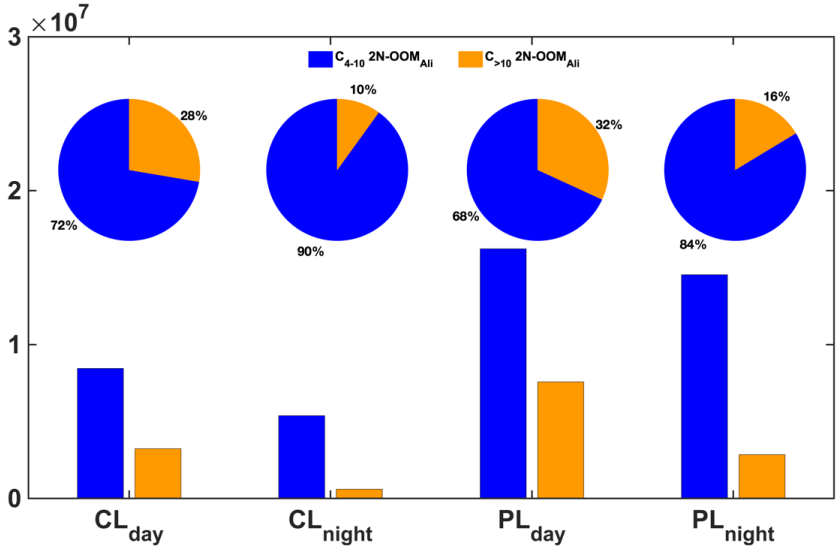

Figure 3

https://doi.org/10.5194/acp-2022-774
Preprint. Discussion started: 17 November 2022

Atmospheric Chemistry and Physics Discussions

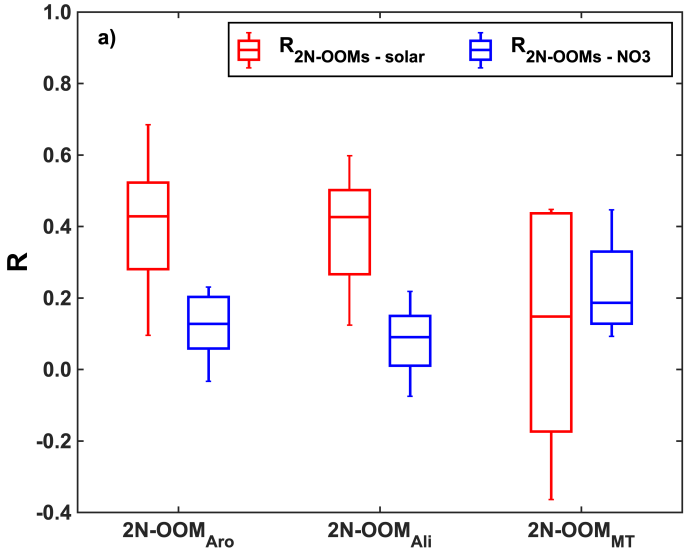

Figure 4a

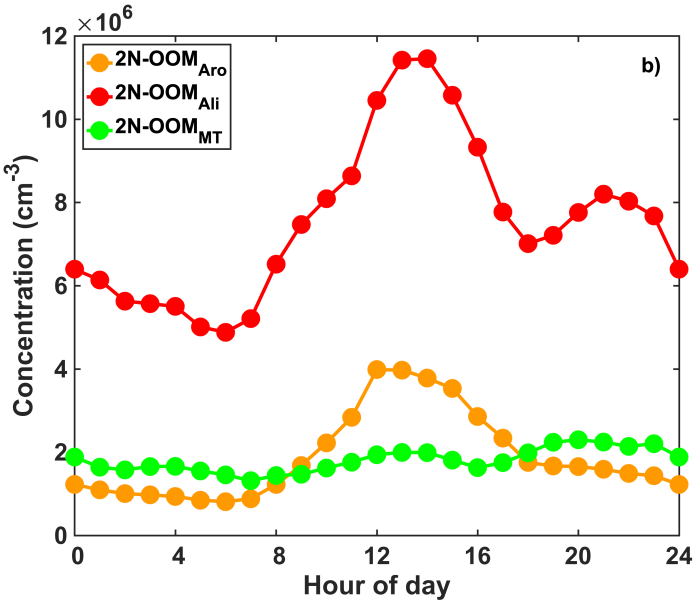

Figure 4b

https://doi.org/10.5194/acp-2022-774
Preprint. Discussion started: 17 November 2022

Atmospheric Chemistry and Physics Discussions

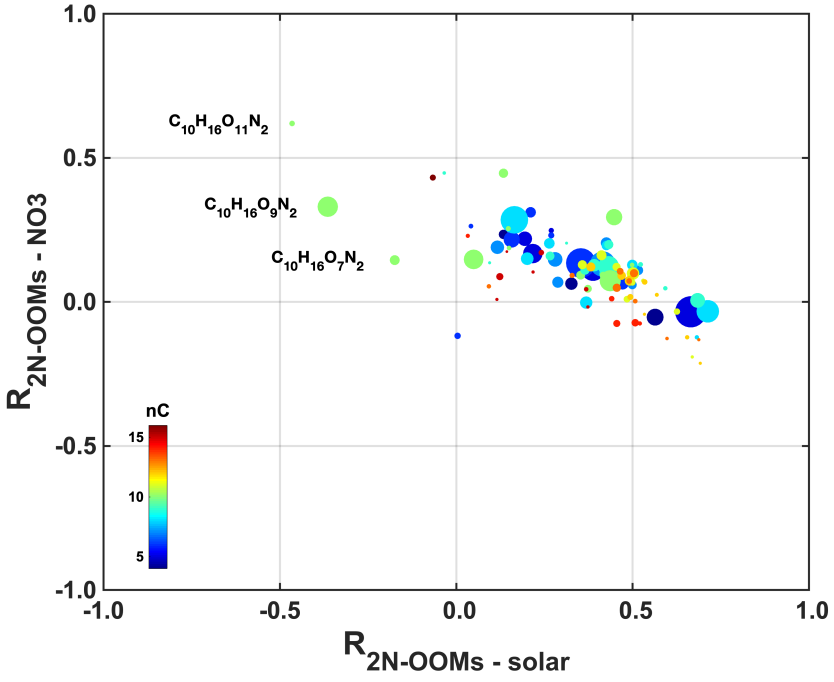

Figure 5

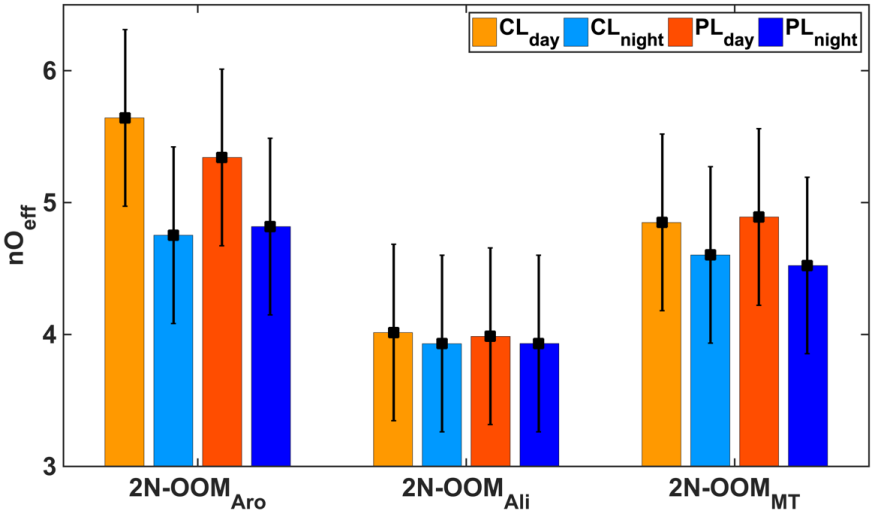

Figure 6

https://doi.org/10.5194/acp-2022-774
Preprint. Discussion started: 17 November 2022

Atmospheric Chemistry and Physics Discussions

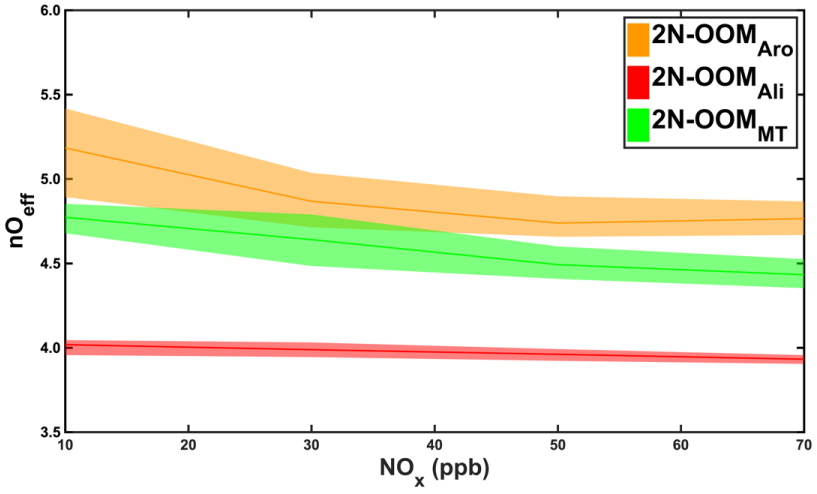

Figure 7